Generation of radioisotopes for medical applications using high-repetition, high-intensity lasers

Katarzyna Liliana Batani*[1], M.R.D. Rodrigues,[2] A. Bonasera**,[2], M. Cipriani,[3] F. Consoli,[3] F. Filippi,[3] M. Scisciò,[3] L. Giuffrida,[4] V. Kantarelou,[4] S. Stancek***,[4] R. Lera,[5] J.A. Pérez-Hernández,[5] L. Volpe,[5] E. Turcu[X,6] M. Passoni,[7] D. Vavassori,[7] D. Dellasega,[7] A. Maffini,[7] M. Huault,[8] H. Larreur+,****,[8] L. Sayo,[9] T. Carriere,[9] P. Nicolai,[9] D. Raffestin,[9] D. Singappuli,[9] D. Batani[9]

[1] *Institute of Plasma Physics and Laser Microfusion (IPPLM), Warsaw, Poland*
[2] *Cyclotron Institute, Texas A&M University, College Station, Texas 77840, USA*
[3] *ENEA, Nuclear Department, C.R. Frascati, Frascati, Italy*
[4] *ELI Beamlines Facility, The Extreme Light Infrastructure ERIC, Dolni Brezany, Czech Republic*
[5] *Centro de Láseres Pulsados (CLPU), Villamayor, Spain*
[6] *UKRI/STFC Central Laser Facility, Rutherford Appleton Laboratory, Harwell Campus, Didcot, OX11 0QX, UK*
[7] *Politecnico di Milano, Dipartimento di Energia, via G. Ponzio 34/3, Milano, Italy*
[8] *Departamento de Física fundamental, Facultad de Ciencias, Universidad de Salamanca, 37008 Salamanca, Spain*
[9] *CELIA - Centre Lasers Intenses et Applications, Université de Bordeaux, Domaine du Haut Carré, 43 Rue Pierre Noailles, 33405 Talence, France.*

** Corresponding author katarzyna.batani@ifpilm.pl*
** Also at Laboratori Nazionali del Sud-INFN, Catania-Italy
***** Also at Joint Laboratory of Optics of Palacky University and Institute of Physics of Academy of Sciences of the Czech Republic, Faculty of Science, Palacky University, Olomouc, Czech Republic
**** Also at HB11 Energy, Australia
+ Also at *CELIA*
[X]Also at Extreme Light Infrastructure: Nuclear Physics (ELI-NP), Reactorului Street, No. 30, Magurele-Bucharest, 077125, Romania

This peer-reviewed article has been accepted for publication but not yet copyedited or typeset, and so may be subject to change during the production process. The article is considered published and may be cited using its DOI.

10.1017/hpl.2024.92

Abstract

We used the PW, high repetition laser facility Vega3 at CLPU in Salamanca, with the goal of studying the generation of radioisotopes using laser-driven proton beams. Various types of targets have been irradiated, including in particular several targets containing boron to generate α-particles through the hydrogen-boron fusion reaction. We have successfully identified γ-ray lines from several radioisotopes created by irradiation using laser-generated α–particles or protons including ^{43}Sc, ^{44}Sc, ^{48}Sc, ^{7}Be, ^{11}C, and ^{18}F. We show that radioisotopes generation can be used as a diagnostic to evaluate α-particles generation in laser-driven proton-boron fusion experiments. We also show the production of $\approx 6 \cdot 10^6$ ^{11}C radioisotopes and $\approx 5 \cdot 10^4$ ^{44}Sc radioisotopes per laser shot. This result can open the way to developing laser-driven radiation sources of radioisotopes for medical applications.

Introduction

The generation of laser-driven particle sources is a current hot topic in physics research with implications, which go from laser driven fusion (and in particular the proton-driven fast ignition approach to inertial fusion [1]) to the realization of several societal or industrial applications [2].
Also, in recent years, high yields of α-particles have been observed from laser-driven hydrogen-boron fusion experiments, opening the possibility to develop a novel approach to high-brightness α-particle sources [3], [4], [5], [6]. These experiments are based on the hydrogen-boron fusion reaction [7], [8]:

$$p + {}^{11}B \rightarrow 3({}^{4}He) + 8.7\ MeV \qquad (1)$$

and have used two different, mainstream schemes: pitcher-catcher configuration (Fig. 1) and in-target irradiation. In the in-target irradiation scheme, the laser beam directly irradiates the boron target (containing hydrogen impurities) [9], [10], [11], [12]. Here, both boron and hydrogen nuclei are accelerated by various mechanisms (including laser hole boring) to finally react releasing the three α-particles.
In the pitcher-catcher scheme, the laser irradiates a pitcher (usually Al or plastic thin foils) producing a proton beam, which is sent onto the catcher, a secondary boron target where the pB reactions take place [13], [14], [15], [16]. Most experiments within this approach used high-energy, high-power laser beams to produce a bright source of protons through the mechanisms of Target Normal Sheath Acceleration (TNSA) [17], [18], [19], [20], [21].

One critical issue is however how to measure the α-yield in a reliable way. The most common diagnostic used in such experiments relies on solid state nuclear track detectors (CR39) [22] and α-particles identification might be a problem due to the simultaneous emission of many ion species from the laser-irradiated targets. Many other diagnostics used in these experiments (Thomson parabolas, Time-of-Flight detectors, …) are also prone to this problem (for a full discussion on the topic see e.g. [23], [24], [25]).
There is indeed another important issue: CR39 and other diagnostics only measure the α-particles escaping the targets, however due to their very short propagation range in solid density matter most α-particles are unable to emerge and are indeed trapped inside the boron target.

Therefore, alternative diagnostic approaches are useful to validate experimental results. One of such novel approaches can be the detection of radioactive isotopes produced in the targets by

https://doi.org/10.1017/hpl.2024.92 Published online by Cambridge University Press

secondary nuclear reactions [23], [26], [36]. Most of the produced radioisotopes are characterized by γ-ray emission, therefore the type and number of produced radioisotopes can be characterized by γ-ray spectroscopy, for instance using a calibrated HPGe detector. The number of proton boron fusion reactions which took place in the target can then be retrieved by the knowing branching ratio between the pB reaction and the reaction which produced the radioisotopes. Of course, γ-rays can measure the total number of reactions which took place inside the target, so there is no "escaping issue" as for α particles and CR39.

Apart from the diagnostic use, the generation of radioisotopes in laser-driven experiments can be very interesting in itself, in particular for producing radioisotopes for medical applications in therapy or diagnostics, in particular PET (Proton Emission Tomography). Radioisotopes used in medicine are currently produced by neutron irradiation in dedicated research reactors, or by proton irradiation using cyclotrons. In principle, laser-driven sources are able to produce energetic protons and neutrons, and they could be used as a complementary technology to generate radioisotopes for diagnostics and medical treatment [27], [28]. In addition, it is also possible to consider radioisotope production using α-particles produced by laser-driven proton boron fusion. Today radioisotopes from α-particles sources are not very used in the medical domain because, even if often they have very interesting properties, only few cyclotrons in the world are able to accelerate α-beams with adequate energy and intensity for their production. Usually, the reactions which produce such radioisotopes show maxima in cross sections for energies higher than 10 MeV [29]. Only dedicated cyclotrons such as ARRONAX [30] or U-120M [31] can produce high-flux of α-particles with energies higher than 10 MeV. The cost and the complexity of such dedicated cyclotrons, as well as the need for extensive radioprotection, strongly limit the spread of such technology and of related radioisotopes.
This is the case for instance of α-emitters like ^{211}At. The current supplies for medically useful α-emitters like ^{211}At are limited by naturally isolated by-products from weapons development and the actual level of production is only sufficient for preclinical studies and limited clinical trials. ^{211}At can also be produced by the irradiation of ^{209}Bi with α-particles [32] which could be realized using laser-driven α-particles sources.
Concerning PET, recently, there has been significant interest in the radionuclides of scandium: ^{44}Sc ($T_{1/2}$= 3.87 h) and ^{43}Sc ($T_{1/2}$=3.89 h) as tracers for PET imaging. ^{43}Sc and ^{44}Sc can be produced by irradiating natural calcium with α-particles from cyclotrons, as already shown by IChTJ group [33], [34] in the Heavy Ion Laboratory of Warsaw University. Alternatively, ^{43}Sc can be produced by irradiating natural Ca with protons, but in this case ^{44}Sc is also produced.

In any case, it is well known that the demand for radioisotopes is rapidly increasing, for both therapy and diagnostics, so there exists a strong societal need of developing new approaches to increasing radioisotope production to meet increasing demand [35]. Therefore, it is very important to study the possibility of producing radioisotopes by laser-irradiation and, in particular, using laser-driven sources of α-particles based on the proton boron fusion reaction.

In conclusion, this paper addresses two different but related points: 1) the use of radioisotopes as a diagnostic of α-particles generation in laser-driven proton-boron fusion experiments, and 2) the feasibility of producing medical radioisotopes using laser-generated protons or α-particles.

https://doi.org/10.1017/hpl.2024.92 Published online by Cambridge University Press

Experimental set-up

The experimental investigation was carried out in March 2023 at the Centro Laseres Pulsados (CLPU) in Salamanca, Spain, using the short-pulse high-intensity laser VEGA 3.

The laser is operating at wavelength λ= 810 nm with the pulse duration τ = 200 - 250 fs and energy of about 25 J. The laser incidence angle on the pitcher target was $\Theta = 12^{o}$, providing on target focal spot size (FWHM) of 12 µm. The temporal contrast was about 2×10^{-5} at 1ps before the main pulse and below 10^{-5} at 5ps.

Although the laser Vega3 can work at repetition rates up to 1 Hz, we did not use such high repetition rate in our experiment mainly due to the need of performing an accurate alignment of each pitcher target before laser shots. We made a shot every 2 min, which compared to many experiments with high intensity lasers can still be considered as a relatively high repetition frequency.

Notice that we have on purpose opted for a non-optimal temporal compression of the VEGA3 laser pulse. Indeed, the full compressed duration (~30 fs) is not optimal for proton acceleration and a longer pulse is more efficient. We experimentally found that proton energy and proton number were optimized for pulse durations of 200 - 250 fs [36].

The experiment was performed in the pitcher-catcher configuration (see Fig. 1). We used a remotely controlled target holder containing tens of pitcher foils producing protons after each shot. Such protons were sent on the same catcher in order to accumulate tens of shots and produce a bigger and more easily measurable quantity of radioisotopes. We irradiated several kinds of catcher targets: pure boron (B), boron nitride (BN), ammonia borane (BNH_6) and calcium silicate (Ca_2SiO_4).

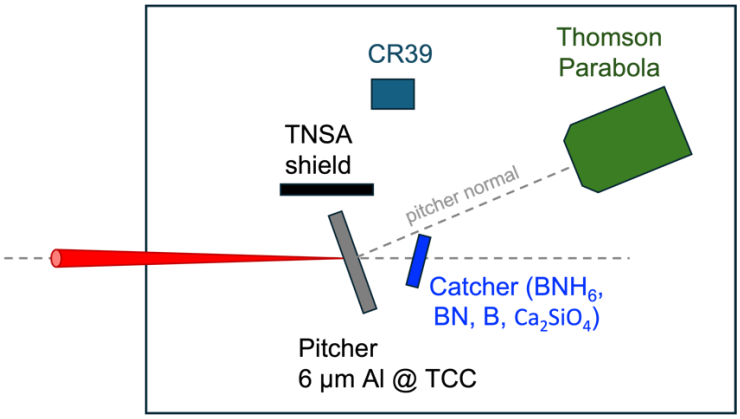

Fig. 1: Scheme of the experimental set-ups used in the experiment. In the configuration with BNH_6 catcher the distance pitcher-catcher was 2 cm, the distance catcher-CR39 was 52 cm, ~~the angle between laser propagation axis and catcher normal was 88.4°, and~~ the angle between laser propagation and catcher normal was 50°. The TNSA shielding prevented protons and other ions emitted from the pitcher to reach the CR39.

Produced radioisotopes were measured using a HPGe γ-ray detector while other diagnostics were used to characterize the proton and the α–particle generation (including CR 39 foil, Thomson parabola spectrometer, time of flight). The general experimental set-up is presented in Fig. 1.

The Thomson parabola spectrometer was used to characterize the spectrum of TNSA protons emitted from the pitcher in shots where the catcher was not present. For a detailed experimental setup of laser and diagnostics see [36], [37], which also describe the results on proton and α particle

https://doi.org/10.1017/hpl.2024.92 Published online by Cambridge University Press

generation. The results described in the paper [37] were acquired during the same experiment. Although the pitcher-catcher scheme was also used, Ref. [37] focuses on the hole-boring scheme (i.e. when the laser directly irradiates the target) and addresses the problem of cross-validation of experimental results and detailed computer simulations.
In this paper, we instead just use the pitcher-catcher configuration, which is more adapted to the production of radioisotopes and in particular we describe the results obtained with ammonia borane and calcium silicate catchers, as an example of the possibilities, and the challenges, offered by the laser-driven approach in production of medical radioisotopes.

Characterization and calibration of Germanium γ-ray detector

In the experiment, we used a High Purity Germanium (HPGe) γ-ray detector equipped with a DSA-1000, 16K channel integrated Multichannel Analyzer and cooled with liquid nitrogen (LN2) at 77 K. The housing of the detector was made of passive iron shield with 15 cm in all directions, screening it from external radiation sources, and the samples had to be positioned inside the same housing.
A fundamental point for the interpretation of the experimental measurement is the characterization and calibration of the spectrometer. We used 3 different γ-radiation sources: ^{137}Cs (emitting a γ line at 661.657 keV), ^{60}Co (emitting two lines at 1173.228 keV and 1332.492 keV), and a mixed source of ^{155}Eu (86.540 keV and 105.30 keV) and ^{22}Na (511.00 keV and 1274.54 keV).

The first step is the calibration with respect to photon energy, i.e. the relation between the analyzer channel (pixel) and the energy of the emitted lines. Fig. 2 presents the energy calibration of the HPGe γ-ray detector showing a linear relationship between photon energy and channel (pixel).

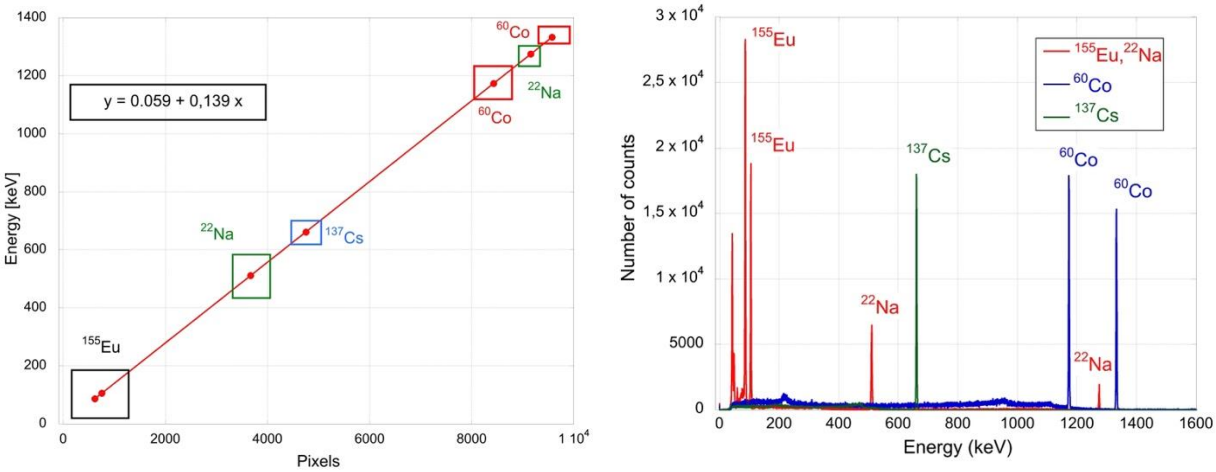

Fig. 2: Energy calibration of the HPGe detector, left) channel - energy relation; right) superposition of the spectra obtained with the radioactive sources.

The second point is establishing a relation between the number of counts and the activity of the sources, i.e. determine the *Detection efficiency*, i.e. the relation between radioisotope activity and recorded counts. In order to do this, we must take into account:
1) the decay of source activity since the time the sources were acquired:

$$N(t) = N_0\, exp(-\lambda\, t) = N_0\, exp\left(-\ln(2)\frac{t}{\tau_{1/2}}\right) \qquad (2)$$

https://doi.org/10.1017/hpl.2024.92 Published online by Cambridge University Press

2) The activity related to each specific γ–ray energy, that is obtained by multiplying the source activity by the γ emission probability, represented as "γ Line Activity".

The results of these calculations are shown in table 1.

Energy [keV]	Source	Isotope	Initial activity [kBq]	Half life [y]	Date of purchase	Spent time [y]	Activity March 2023 [kBq]	Probability	Line Activity Today [kBq]
43.375	$^{22}Na^{155}Eu$	^{155}Eu	37.000	4.7600	7-7-2011	11.750	6.6876	0.12000	0.80251
60.250	$^{22}Na^{155}Eu$	^{155}Eu	37.000	4.7600	7-7-2011	11.750	6.6876	0.012200	0.081589
86.540	$^{22}Na^{155}Eu$	^{155}Eu	37.000	4.7600	7-7-2011	11.750	6.6876	0.30854	2.0634
105.30	$^{22}Na^{155}Eu$	^{155}Eu	37.000	4.7600	7-7-2011	11.750	6.6876	0.21100	1.4111
511.00	$^{22}Na^{155}Eu$	^{22}Na	37.000	2.6000	7-7-2011	11.750	1.6146	1.7980	2.9031
661.66	^{137}Cs	^{137}Cs	9.8000	30.170	27-10-2021	1.3000	9.5117	0.85000	8.0849
1173.2	^{60}Co	^{60}Co	37.000	5.2700	23-4-2016	6.9100	14.908	0.99850	14.886
1274.5	$^{22}Na^{155}Eu$	^{22}Na	37.000	2.6000	7-7-2011	11.670	1.6494	0.99940	1.6484
1332.5	^{60}Co	^{60}Co	37.000	5.2700	23-5-2016	6.8300	15.071	0.99983	15.068

Tab. 1: Calculation of the activity corresponding to each of γ–ray energy in the spectra emitted by the calibration sources.

We then calculated the Peak Detection Efficiency D as the ratio between the Line Activity (in kBq) and the recorded number of counts in the γ-ray line, recorded during a 5-minute acquisition.

$$D = \frac{Line\ activity\ \gamma}{Number\ of\ counts} \qquad (3)$$

The results of the calculations are shown in Fig. 3 where the photon energy is in keV, and the line activity is measured in kBq. We see that the peak detection efficiency D depends on γ–ray photon energy and that the relation is practically linear (and passing through the origin, i.e. D is proportional to $h\nu$).

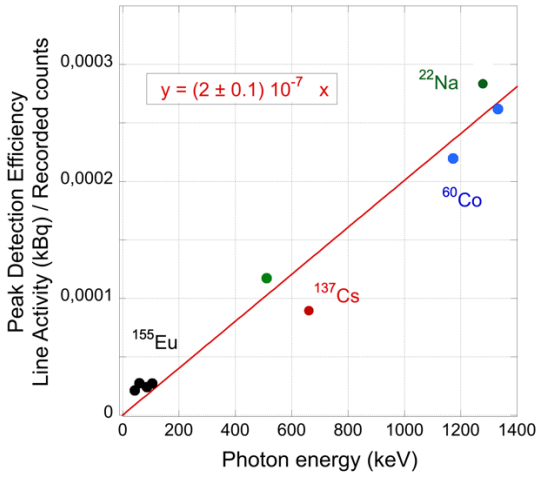

https://doi.org/10.1017/hpl.2024.92 Published online by Cambridge University Press

Fig. 3: Activity calibration line showing the Peak Detection Efficiency D as a function of γ–ray photon energy (considering counts recorded during a 5-minute acquisition).

We also performed a sensitivity scan by displacing the radioactive source inside the container with respect to the central position (the source placed exactly on the vertical axis of the detector at a fixed distance of 1 cm). Fig. 4 and 5, respectively show the results of displacing the sources in the vertical

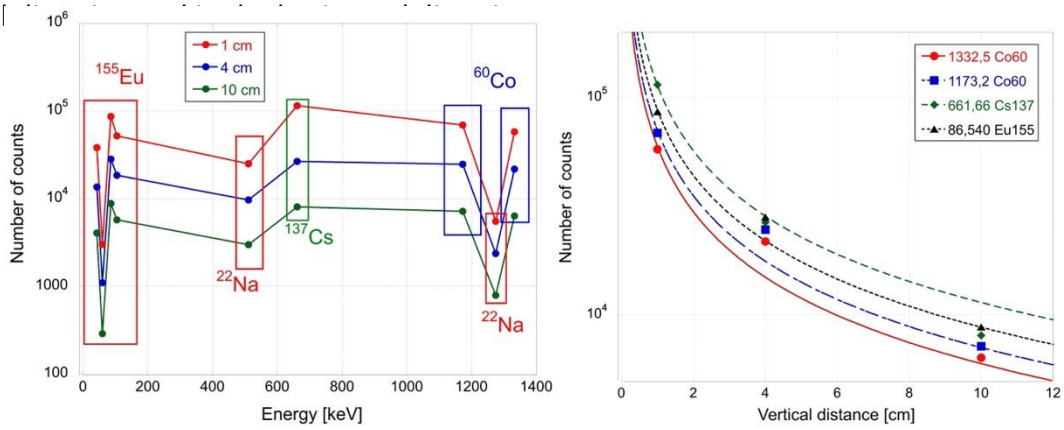

Fig. 4: γ-ray detector sensitivity variation when displacing the sources in the vertical direction with respect to the detector.

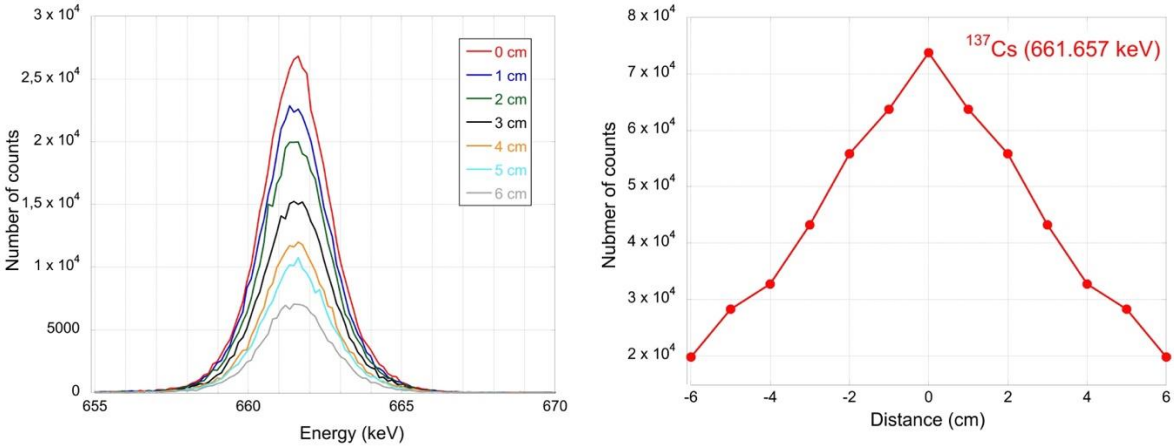

Fig. 5: γ-ray detector sensitivity variation when displacing the sources in the horizontal direction with respect to the detector.

The number of recorded counts approximately scales inversely proportional with respect to the vertical displacement (i.e. $Counts \approx 1/d$) and linearly with respect to the horizontal displacement. This measurement is important because it allows estimating the error in number of recorded counts which corresponds to a non-perfect positioning of the source or to different source geometry. For instance, a displacement of 1 cm in the lateral direction implies a reduction of 10% in counts, while a displacement of 1 cm in vertical direction implies reduction of 50% in counts.

In order to analyze the γ-ray spectra, we performed an accurate measurement of the background (due to cosmic rays or other sources) with the same detector, and we then subtracted such background from our experimental spectra.

A final question related to the calibration of the spectrometer concerns the impact of Compton scattering on the recorded spectra. Not all the emitted γ-photons at one energy $h\nu$ are found in the

https://doi.org/10.1017/hpl.2024.92 Published online by Cambridge University Press

corresponding line but many undergo Compton scattering (at an angle θ) with the electrons in the detector material after which they might escape the detector volume and therefore are recorded as photons at lower energy $h\nu'$:

$$\frac{1}{h\nu'} - \frac{1}{h\nu} = \frac{1}{mc^2}(1 - cos\theta) \qquad (4)$$

Monte Carlo simulations are needed to give a quantitative evaluation of this effect (depending on detector size and geometry). However, in our set-up, we can get an estimation by using the single line spectrum emitted by the ^{137}Cs source (for multiple line spectra the situation is more complex due to the superpositions of some lines to the Compton shoulder and the superposition of Compton shoulders from different lines).

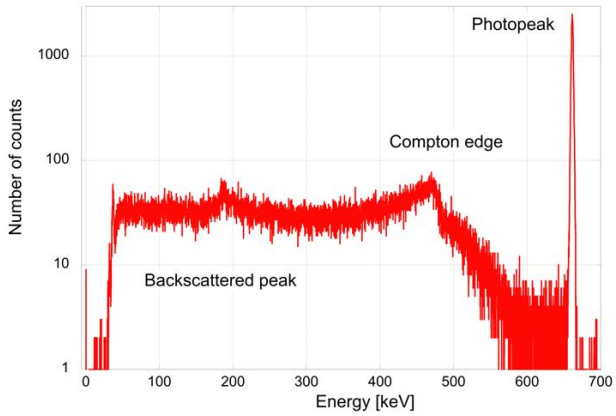

Fig. 6: Compton shoulder in the spectrum recorded with the ^{137}Cs source having a single line source at 662 keV in Logarithmic scale.

Fig. 6 shows the spectrum of ^{137}Cs in logarithmic scale. Although on a linear scale the Compton shoulder seems small, due to its large energy range, it indeed contains more photons than the line peak. The ratio between total number of counts and counts in the peak is ≈ 3.5.
This factor is anyway naturally included in the calibration, which relates the number of counts recorded in the main γ–ray line to the total activity of the source (i.e. including the decay which will end up in the Compton shoulder).

Radioisotope generation using BNH_6

We placed an Ammonia-Borane pellet (BNH_6) on the rear side of the Al pitcher (6 µm in thickness) at a distance of 2 cm. The pellet had a diameter of 12 mm and a thickness of 1.2 mm, and it was produced by Chris Spindloe and coworkers [38] by compression of commercially available BNH_6 powder. A detailed discussion of the targets can be found in [39], [new_reference]. The sample was inclined under 50° to the laser propagation axis. After irradiation the sample was placed in the HPGe detector and acquisitions were done every 5 minutes (accumulating the signal for 5 min). Fig. 7 shows the accumulated γ-ray spectrum recorded after the irradiated over the period of 1 hour and 40 minutes and measured for 60 minutes, showing a strong peak at 511 keV.

https://doi.org/10.1017/hpl.2024.92 Published online by Cambridge University Press

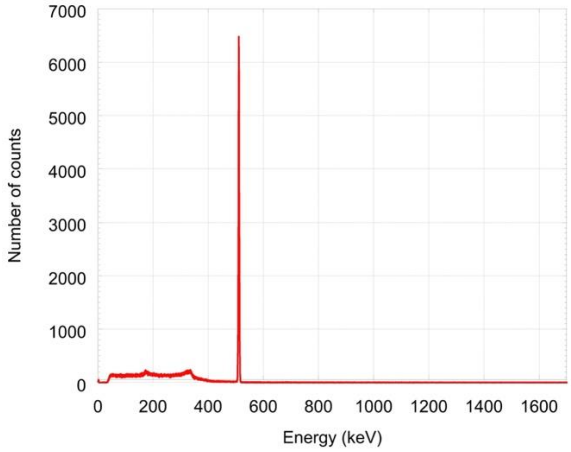

Fig. 7: γ–ray spectrum recorded from a BNH_6 (Ammonia-Borane) pellet irradiated with 31 laser shots (accumulation time over 1 hour and 40 minutes).

Since the 511 keV line is due to annihilation of positrons emitted from radioisotopes with the electron in the material, it is typical of any β+ emitter. In order to recognize the origin of such emission we must then analyze the time decay of the line and identify it with the lifetime of a specific radioisotope.

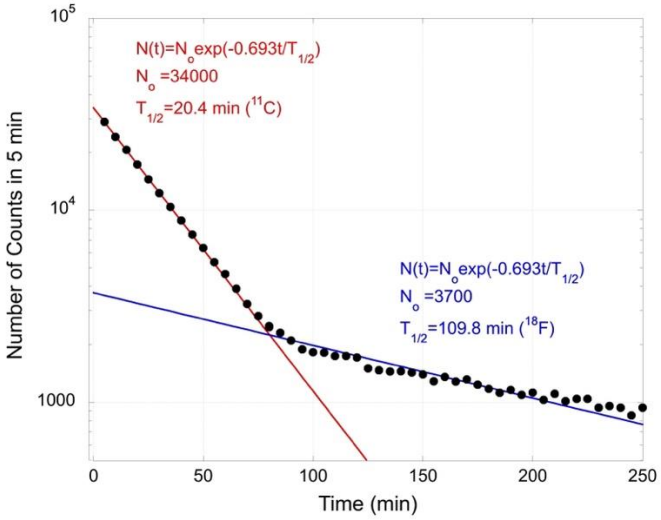

Fig. 8: Count decay in time of the 511 keV line from the irradiated BNH_6 (Ammonia-Borane) pellet. The time 0 in this graph corresponds to the beginning of the measurement with the HPGe detector, typically about half an hour after the end of the irradiation (due to the time needed to vent the chamber, extract the sample, insert it in the HPGe detector)

In Fig. 8, we recognize two different decay slopes. The first corresponds to a half-life $T_{1/2} = 20.4$ min and the second one to $T_{1/2} = 109.8$ *min*. This allows to identify the first one as the decay of ^{11}C and the second one as the decay of ^{18}F. ^{11}C decays as:

$$^{11}C^{*} \longrightarrow {}^{11}B + e^{+} + n \qquad (5)$$

And is produced by the reaction:

$$p + {}^{11}B \longrightarrow {}^{11}C^{*} + n - 2.765\ MeV \qquad (6)$$

^{18}F decays as:

$$^{18}F \longrightarrow {}^{18}O + e^{+} + n \qquad (7)$$

https://doi.org/10.1017/hpl.2024.92 Published online by Cambridge University Press

and it can either be produced by the reaction:

$$\alpha + {}^{14}N \longrightarrow {}^{18}F^{*} + \gamma + 4.415\ MeV \qquad (8)$$

from the α-particles generated by the proton boron fusion reaction reacting with the nitrogen in BNH_6, or from the reaction:

$$^{18}O + p \longrightarrow {}^{18}F^{*} + n + 2.44\ MeV \qquad (9)$$

from the impurities in the sample (i.e. absorbed water). Of course, the quantity of oxygen in our sample is much less than nitrogen, however the flux of protons is much higher that the number of α-particles (usually in this kind of experiments the ratio between α-particles and protons is of the order of 10^{-4} [12], [15], [16]). Hence in our case the most probable origin of ^{18}F is from oxygen impurities (i.e. from water).
Let's note that in principle we could also observe the 511 keV from the decay of $^{13}N^{*}$, another $\beta+$ emitter which can either be produced by the reaction $\alpha + {}^{10}B \longrightarrow {}^{13}N^{*} + n + 1.06$ MeV, or by the reaction $p + {}^{16}O = {}^{13}N^{*} + \alpha - 5.22$ MeV. However, due to the very short lifetime of ^{13}N ($T_{1/2}$ = 9.97 min) we could not see the signature of its decay in our measurements.

Starting from the graph in Fig. 8 and the calibration line of Fig. 3 we can evaluate the activity and number of produced ^{11}C isotopes. Fig. 8 shows that the number of counts recorded during 5 min is $N_o \approx 34000$ at t=0. At the photon energy of 511 keV, which is the same of the line from ^{22}Na, the detection efficiency is:

$$D = \frac{Activity\ (kBq)}{Counts} \approx 0.0001 \qquad (10)$$

From which we recover an activity of 3.4 kBq obtained with 31 shots on target. The relation between activity, the decay constant λ, the lifetime $T_{1/2}$, and the number *N* of radioisotopes is:

$$A = N\lambda \qquad \lambda = \frac{0.693}{T_{1/2}} \qquad (11)$$

which for ^{11}C gives $\lambda = 5.66 \cdot 10^{-4}$ s^{-1}, from which the number of ^{11}C radioisotopes can be estimated as:

$$N_{31\#} = 6.0 \cdot 10^{6} \qquad (12)$$

As specified before, this number corresponds to the beginning of the measurement with the HPGe detector, typically about half an hour after the end of the irradiation (due to the time needed to vent the chamber, extract the sample, etc.). By correcting for the decay rate, we see that the number of counts, which would be recorded just after the end of the irradiation would increase by a factor ≈4.34 thereby yielding ≈ 148000 counts. This corresponds to an activity of ≈15 kBq.

https://doi.org/10.1017/hpl.2024.92 Published online by Cambridge University Press

In reality such number must also be corrected to take into account that the time needed to accumulate 31 shots was ≈1 hour, thereby there was a significant decay of ^{11}C during the irradiation itself. The calculation, performed in Appendix A, shows that realizing the 31 shots in a very short time compared to the lifetime ($T_{1/2}$ = *20.4 min*) would have provided an increase of a factor ≈ 2.42, bringing the total production of ^{11}C radioisotopes to $\approx 6.4 \cdot 10^7$ and the total activity to ≈36 kBq. Hence, we estimate that one laser shot thus produces about $2 \cdot 10^6$ ^{11}C, or an activity of > 1 kBq.

Another interesting question is how we compare the number of generated ^{11}C isotopes and α–particles, that is the number of fusion reactions taking place. This is relevant to establishing the capability of using γ–ray emission from ^{11}C as a diagnostics of hydrogen boron fusion in addition to classical CR39 detectors. The number of created α-particles and ^{11}C has been evaluated using a simple python software validated against the results of more complex Monte Carlo simulations (as described in Appendix B). The calculation uses the experimentally measured proton spectrum as input [the spectrum is shown in Appendix B].
This shows that in each laser shot $\approx 0.97 \cdot 10^6$ ^{11}C are generated, i.e. the experimental result is indeed close to the calculation (within a factor of two).

The experimental evaluation of α–particle yield is more difficult being based on analysis of CR39 foils [22], [23], [40], which contains a certain degree of uncertainty and, of course, only measures the α-particles escaping the target. The number of escaping α-particles is evaluated in Appendix B and corresponds to $\approx 1.2 \cdot 10^6$ particles exiting the target from the front side per laser shot, or about $\approx 0.84 \cdot 10^6$ α-particles with energy > 1.57 MeV.
For comparison the analysis of CR39 (see Appendix C) provides a number of $5 \cdot 10^5$ α-particles with energy ≥ 1.57 MeV per solid angle and per laser shot. Assuming an isotropic generation over the 2π solid angle corresponding to the "front side", we get an estimation of $3 \cdot 10^6$ α–particles of energy >1.57 MeV. This number corresponds to what is measured when a 5 µm Al foil filter is placed in front of the CR39 detector. This filter transmits α–particles of energy >1.57 MeV but prevents a significant contamination from other laser accelerated ions.
The theoretical estimation is therefore a factor of 3 below the experimental one (the difference might be largely due to the hypothesis of isotropic generation over a 2π solid angle).
If we look at the ratio of ^{11}C to α-particles (with energy > 1.6 MeV), we see that:

$$\left(\frac{\alpha}{^{11}C}\right)_{exp} = \left(\frac{3 \cdot 10^6}{2 \cdot 10^6}\right)_{exp} \approx 1.5 \qquad \left(\frac{\alpha}{^{11}C}\right)_{cal} = \left(\frac{0.84 \cdot 10^6}{0.97 \cdot 10^6}\right)_{cal} \approx 0.9 \qquad (13)$$

This shows that, within the limit of precision of the present experiment, the measured activity of ^{11}C is in fair enough agreement with the measured α–particle yield and can indeed provide a way to estimate the total number of hydrogen-boron fusion reactions. The excess number of α-particles with respect to ^{11}C might be possibly due to the fact that the CR39 measurement is somewhat polluted by the presence of other ions coming from the catcher [36]. As mentioned before the theoretical evaluation from Appendix B predicts $1.2 \cdot 10^6$ α-particles escaping the catcher from the front side and a total α-particle yield of $1.11 \cdot 10^7$, i.e. in our experimental configuration about 90% of α-particles remain trapped inside the catcher. This is similar to what already shown in M. Scisciò et al. [36] in the case of natural B catchers.
Taking into account that one fusion reaction releases 3 α-particles, we estimate that in this configuration we have produced $\approx 4 \cdot 10^6$ hydrogen boron fusion reactions per laser shot.

https://doi.org/10.1017/hpl.2024.92 Published online by Cambridge University Press

Radioisotope generation using Calcium silicate

The irradiation of calcium can bring to the production of Scandium radioisotopes, which are very interesting for present, and even more for future, medical applications. In particular ^{44}Sc and ^{43}Sc are β^- emitters with short-lifetime (< 4 h) and with simultaneous emission of γ ray only at relatively low energy. For these characteristics, they will produce little collateral damage to healthy cells and are therefore considered as optimal radiation sources for PET imaging.

In the experiment we irradiated Calcium silicate samples (Ca_2SiO_4, sample size: 5 cm×5 cm× 0.5 cm). A thin layer of ^{11}B was deposited on the samples using a PLD technique at Politecnico di Milano. The layer thickness was ≈3 μm and its atomic composition approximately equal to 95-96% ^{11}B and 4-5% O. More details about the PLD system and the characteristics of the boron films can be found in [41], [42]. The goal of this layer was of course to absorb part of the incident proton flux and produce α-particles by the proton-boron fusion reactions. Such α-particles could then induce the formation of radioisotopes in calcium silicate.

The samples were placed behind the Al pitcher (6 μm) inclined by 12° with respect to the laser propagation axis, at a distance of 2 cm, and irradiated with 31 laser shots. After irradiation the sample was placed in the HPGe detector and acquisitions were done every 5 minutes (accumulating signal for 5 min). The accumulated spectrum is shown in Fig. 9 in the range $950 - 1700\ eV$. It shows the presence of several γ-ray lines from ^{44}Sc and ^{48}Sc. At lower energy we find the line at 511 keV, due to positron annihilation.

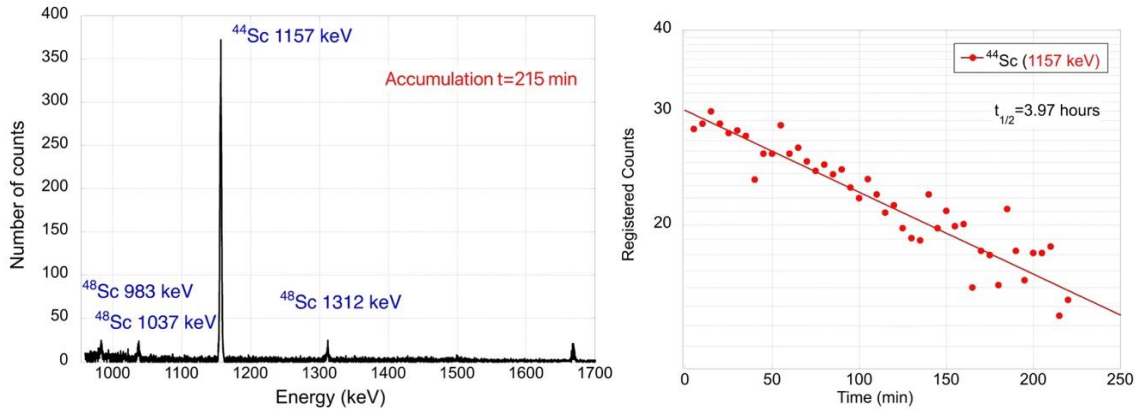

Fig. 9: left) Recorded γ-ray spectrum in the range $h\nu > 950\ keV$. The line at 1669 keV corresponds to the simultaneous absorption of photons at 1157 keV and 511 keV; right) Decay of the emission line at 1157 keV in time.

Similar spectra have already been identified in literature [43], [44], [45] (but not from laser-generated radioisotopes). As an additional proof, we measured the decay time of the line at 1157 keV, as shown in Fig. 9 (right). The measured lifetime agrees well, within error bars, with the lifetime of ^{44}Sc.

Scandium radioisotopes can be produced by irradiation of natural calcium with protons or α-particles as shown in Table 2 [46].

Radioisotope	Lifetime	Production	Decay
^{43}Sc	3.89 h	$\alpha + {}^{40}Ca \rightarrow {}^{43}Sc + p$ $\alpha + {}^{40}Ca \rightarrow {}^{43}Ti + n$, ^{43}Ti ($T_{1/2}$ = 509 ms) $\rightarrow {}^{43}Sc + e^+ + n$ $p + {}^{43}Ca \rightarrow {}^{43}Sc + n$ $p + {}^{44}Ca \rightarrow {}^{43}Sc + 2n$	$^{43}Sc \rightarrow {}^{43}Ca + e^+ + \bar{\nu}_e$

https://doi.org/10.1017/hpl.2024.92 Published online by Cambridge University Press

^{44}Sc	3.97 h	p + ^{44}Ca → ^{44}Sc + n	^{44}Sc→ ^{44}Ca + e^+ + $\overline{\nu_e}$
^{48}Sc	43.67 h	p + ^{48}Ca → ^{48}Sc + n α + ^{46}Ca → ^{48}Sc + 2n	^{48}Sc→ ^{48}Ti + e^- + ν_e

Tab. 2: Production and decay chain for the scandium radioisotopes observed in our experiment.

^{44}Sc is produced by the reaction of protons with ^{44}Ca. In our case, the isotope ^{48}Sc is likely produced also by protons rather than α–particles, first of all because, as already written before, in laser-driven proton-boron fusion experiments the ratio of produced α-particles to protons is ≈ 10^{-4}, and second because ^{48}Ca is much more abundant than ^{46}Ca representing only 0.004% of natural calcium (see Table 3).

^{40}Ca	^{42}Ca	^{43}Ca	^{44}Ca	^{46}Ca	^{48}Ca
96.9 %	0.657%	0.135%	2.09%	0.004%	0.187%

Tab.3: Abundance of stable isotopes of Calcium (except ^{48}Ca, which is practically stable with a lifetime of 6.4 · 10^{19} years).

As done for ^{11}C we can evaluate the number of produced radioisotopes starting from the recorded γ–ray spectra. The number of counts recorded at the initial time (see Fig. 9) is ≈ 200. In this case since the lifetime of ^{44}Sc is not as short as ~~short as~~ the one of ^{11}C, the corrections taking into account the decay time are not so important. 200 counts obtained at the beginning of the measurement with the HPGe corresponds to ≈226 counts half an hour before (i.e. at the end of the irradiation) and the correction taking into account the irradiation time implies an additional factor of ≈ 1.05 (see Appendix A). This would bring the total number of counts to ≈ 240.
The detection efficiency approximately corresponds to that obtained from ^{22}Na at energy 1274.5 eV (which is close to the 1157 keV line of ^{44}Sc), i.e. $D \approx 0.00027$ (for 5 min accumulation) which corresponds to an activity A:

$$A\,(kBq) = D \times Counts \approx 0.065\,kBq \qquad (14)$$

with 31 shots on target. The decay constant for ^{44}Sc is $\lambda = 4.76 \cdot 10^{-5}\ s^{-1}$, from which we get:

$$N_{31\#} = \frac{65}{4.76 \cdot 10^{-5}} \approx 1.4 \cdot 10^{6} \qquad (15)$$

Hence, we can estimate a production of ≈ $4.5 \cdot 10^{4}$ radioisotopes per shot.

We also looked for the signature of ^{43}Sc, which emits a γ-ray line at 373 keV. The line was indeed present but very weak and superimposed on the Compton shoulder. In order to get an estimation, we had to remove the contribution of the Compton shoulder and smooth the data to remove noise. The original spectrum and the treated one are shown in Fig. 10.

The low production of ^{43}Sc in comparison to ^{44}Sc is explained by the lower abundance of ^{43}Ca in comparison to ^{44}Ca within the natural calcium material used in the experiment. In addition, the production of ^{43}Sc from α–particles is negligeable, again because of the much smaller number of α-

https://doi.org/10.1017/hpl.2024.92 Published online by Cambridge University Press

particles with respect to protons which balances the fact that ^{43}Ca is only 0.135% of natural calcium (see Table 3).

We also observed a weak emission of γ-ray line at 477 keV from the isotope ^{7}Be, which is produced by the reaction p + ^{10}B → ^{11}C* → ^{7}Be + α (lifetime of 53.22 days).

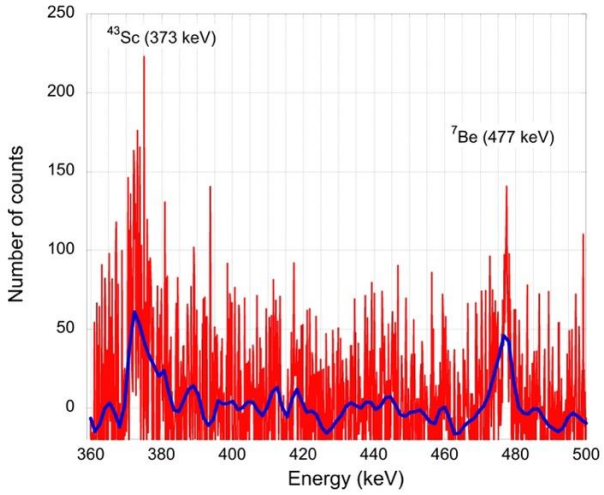

Fig. 10: left) Accumulated γ–ray spectrum from the Ca_2SiO_4 sample in the range 350 keV < $h\nu < 500\ eV$. ^{43}Sc and ^{7}Be γ-ray emission lines are superimposed to the Compton shoulder; right) the same after removing the Compton and after smoothing. The sample was irradiated for 33 min, and the measurement was accumulated over 3h45.

Future perspectives

We have successfully shown the production of radioisotopes in laser-driven experiments. This can be useful potentially for the possibility of producing radioisotopes of interest for medical applications and also for diagnostics purposes (i.e. infer the total number of nuclear reactions taking place in the target). In this case of course we need to greatly improve the yields from laser experiments in order to become competitive with existing tools for radioisotope production.

Currently radioisotopes are produced either in nuclear reactors (by neutrons) or in dedicated cyclotron systems (by protons). A few specific radioisotopes are also produced using Large Heavy Ion Cyclotron systems (like the cited ARRONAX or U-120M), which accelerate He-nuclei, i.e. α-particles. For instance, ARRONAX can produce a current of 70 μA of α–particles. A current of 10 μA corresponds to a flux of α-particles:

$$10\ \mu A \ \rightarrow \quad N_\alpha \Big/ s = \frac{10^{-5}\ C/s}{2 \times 1.6\ \cdot 10^{-19} C} = 3\ \cdot 10^{13}\ \alpha/s \qquad (16)$$

Reaching performances of the order of a few 10 μA of α-particles with lasers is extremely challenging. Today, laser experiments show a maximum of 10^{11} α/sr/shot or about a maximum of 10^{12} α/shot [11], [12]. In order to be comparable such laser-driven source must then work at a repetition rate

https://doi.org/10.1017/hpl.2024.92 Published online by Cambridge University Press

$$f = \frac{3 \cdot 10^{13}\ \alpha/s}{10^{12}\alpha/shot} = 30\ Hz \qquad (17)$$

This requires developing a new generation of ≈ 100 Hz PW laser systems. Although this is a challenging goal, laser technology is indeed already moving in this direction [47]. Also notice that indeed in our experiment, α-particle yield was much lower than those "record" yields.
In reality, even operating less performing laser-driven α–particle sources could still be interesting if laser-driven sources are cheaper and more compact so to be installed in more medical centers and be more diffused in the territory (this is particularly important for short-life radioisotopes, which are the most interesting for medical applications) serving as 'in-hospital' isotope manufacturing for fast administration of short-lived isotopes.

At the same time, in order to increase the number of produced radioisotopes for laser shots, we need to carefully choose target materials. For instance, while in our experiment we produce $4.5 \cdot 10^4$ ^{44}Sc radioisotopes per shot with natural Ca (mixture of ^{44}Ca and other Ca isotopes), we could increase the production by using a target containing only ^{44}Ca. This is likely to increase radioisotope production by a factor 1/2.09% ≈ 50. An even larger increase would be obtained by using a pure ^{44}Ca target instead of a calcium silicate.

It is also clear that for radioisotopes produced by α-particles, a 3-step process (pitcher → catcher → target material) is very ineffective. Many particles are lost at each step, and, above all, most α-particles are confined in the catcher due to the very short propagation range in solid density matter (≈ microns). We therefore need to use mixed targets, where boron (to produce α–particles from protons) and the target material (generating the radioisotopes) are in direct contact. Concerning Sc radioisotopes, interesting materials are indeed calcium silicate or even better calcium hexaboride (B_6Ca).

The other important question concerns the purity of produced radioisotopes. For instance, in the case of Sc, it would be preferable to produce a single radioisotope rather than a mixture of ^{44}Sc, ^{48}Sc, and ^{43}Sc. ^{44}Sc and ^{43}Sc are both used in medicine as source for PET imaging. However, ^{43}Sc is often considered as the "radioisotope of the future" in PET because of its short lifetime and the absence of simultaneous γ-emission at energies high enough to possibly cause radiation damage to human cells (^{43}Sc emits γ rays at 373 keV which is even lower than γ rays emitted by ^{44}Sc at 1157 keV). Pure ^{43}Sc could be obtained by irradiating natural calcium with α-particles. Unfortunately, in experiments with laser driven α–particle sources, the α-particles are always accompanied by a much larger flux of protons which, as in the present experiment, can produce ^{44}Sc by reaction with the isotope ^{43}Ca. Indeed, although ^{43}Ca is only 2.09 % of natural calcium, the α-particles are far less than protons, so this reaction channel is dominant. Using isotopically pure ^{40}Ca would prevent this, however ^{40}Ca is present at 96.9% in natural Ca and it is very difficult to get isotopic concentration above 99.5% [48]. Instead, pure ^{44}Sc could be obtained using protons on isotopically pure ^{44}Ca (the production of ^{43}Sc by the 2*n* reaction being largely minoritarian). In this case, one should consider that present compact cyclotrons used for production of medical radioisotopes have currents of the order of 100 - 150 μA, which is a factor ≈2 above the α-particle current produced by ARRONAX. However, as we said before, the ratio of α-particles to protons in laser-driven experiments for production of particle sources is typically a factor ≈10^4 in favor of protons. To produce 100 μA, a laser which works at 100 Hz repetition frequency should accelerate ≈ $6\ 10^{12}$ protons per laser shot. If the protons have an

https://doi.org/10.1017/hpl.2024.92 Published online by Cambridge University Press

average energy of 10 MeV, the total energy in the proton beam is about 1 J which could imply a laser energy per shot of 10 J assuming a laser to proton conversion efficiency of 10%. Indeed, these numbers represent a reasonable (although optimistic) extrapolation of current performances, which shows how laser-driven proton sources could also be interesting for production of medical radioisotopes.

Conclusions

In our experiment, we have successfully identified γ-ray lines from multiple radioisotopes created by irradiation using laser-generated α or protons. These includes ^{43}Sc, ^{44}Sc, ^{48}Sc, ^{7}Be, ^{11}C, and ^{18}F. With respect to our previous work (ref. [27]) here we focused on radioisotopes of medical interest (^{43}Sc, ^{44}Sc) and we provided an evaluation on how laser-driven source could become competitive for radioisotope production. We also described the HPGe detector and the calibration procedure in detail, and we have also shown a fairly good agreement between data obtained from γ-ray spectroscopy and other diagnostics (CR39). This shows the possibility of using γ–ray spectroscopy as a reliable diagnostic to measure activation of target materials and reaction rates. This can be important for instance for proton-boron fusion experiments where measuring α–particle yields with CR39 has always been an issue.

We have also shown the production of $\approx 6 \cdot 10^6$ ^{11}C radioisotopes and $\approx 5 \cdot 10^4$ ^{44}Sc radioisotopes per laser shot. Again, a proper choice of target material can considerably increase the production rate: this could be pure ^{11}B for ^{11}C production or pure ^{44}Ca for ^{44}Sc production. This result can open the way to developing laser-driven radiation sources of radioisotopes for medical applications.

In this context in the future, we will need to perform experiments which produce a separable quantity of radioisotopes (*first step*), and which matches the doses (MBq) used in medicine (*second step*). These objectives can be achieved both by accumulating a much larger number of shots (i.e. working at high repetition rate), and by optimizing laser parameters, and developing new target materials (e.g. for radioisotopes produced by α-particles target mixing boron and the precursor material of the radioisotope to be produced).

Acknowledgements

We thank the Laser Division and Radioprotection, the Engineering and TIC areas, and the Managing divisions of the CLPU for their valuable support. We thank Chris Spindloe from Scitech Precision Ltd., UK, for providing the ammonia borane targets.

This work has been supported by COST (European Cooperation in Science and Technology) through the Action CA21128 PROBONO (PROton BOron Nuclear Fusion: from energy production to medical applicatiOns). It also has received funding from the European Union's 2020 research and innovation programme under the grant agreement No 101008126 (RADNEXT project) and from the United States Department of Energy under Grant #DEFG02-93ER40773.

SMILEI simulations were performed thanks to granted access to the HPC resources of TGCC under the Allocation Nos. 2023-A0140514117 made by GENCI". We also acknowledge the financial support of the IdEx University of Bordeaux / Grand Research Program "GPR LIGHT", and of the Graduate Program on Light Sciences and Technologies of the University of Bordeaux. L.G. and V.K. acknowledge the support of the Czech Science Foundation through Grant No. GACR24-11398S.

Finally, we acknowledge the support of HB11 Energy, Ltd, Australia, through its Collaborative Science Program. HL and MH acknowledge the direct support of HB11.

https://doi.org/10.1017/hpl.2024.92 Published online by Cambridge University Press

Appendix A: Effect of decay

In the case of short-living elements, one must take into account the decay during the time τ_1 between the end of the irradiation and the beginning of the measurements with the γ-ray spectrometer, but also the decay during the time needed to do all laser shots.

This is important for the case of ^{44}Sc with a lifetime *$T_{1/2}$ = 3.97 h = 238.2 min* and even more for ^{11}C with a lifetime *$T_{1/2}$ = 20.4 min.* In comparison typically $\tau_1 \approx 30$ min. In addition, we were doing a laser shot every 2 min (= τ_2), which means that the total time needed to perform 30 shots is 1 hour (= τ_3).

In this case if N_o is the number of radioisotopes created by a single laser shot, the number of radioisotopes with decay time τ present at the end of the shot series will be, counting from the first to the last shot:

$$N = \left[N_o e^{-(\tau_3/\tau)} + N_o e^{-((\tau_3-\tau_2)/\tau)} + N_o e^{-((\tau_3-2\tau_2)/\tau)} + \cdots + N_o e^{-((\tau_3-n\tau_2)/\tau)}\right]$$
$$= \quad N_o e^{-(\tau_3/\tau)} \sum_{i=0}^{n-1} e^{(\,i\,\tau_2/\tau)} \;=\; N_o e^{-(\tau_3/\tau)} \sum_{i=0}^{n-1} e^{(\tau_2/\tau)^i} \qquad (18)$$

Where τ is related to the lifetime by the relation $\tau = T_{1/2}/0.693 = 1/\lambda$. The last factor is the geometrical sum of terms with ratio $e^{(\tau_2/\tau)}$, and therefore the result is:

$$\frac{1-e^{(\tau_2/\tau)^n}}{1-e^{(\tau_2/\tau)}} = \frac{1-e^{(n\tau_2/\tau)}}{1-e^{(\tau_2/\tau)}} = \frac{1-e^{(\tau_3/\tau)}}{1-e^{(\tau_2/\tau)}} \qquad (19)$$

since of course $n\tau_2 = \tau_3$. Notice that for $\tau_2 \to 0$ (or equivalently for long life radioisotopes for with $\tau \gg \tau_3 > \tau_2$) we get:

$$\sum_{i=0}^{n-1} e^{(\tau_2/\tau)^i} = \sum_{i=0}^{n-1} 1 = n \qquad (20)$$

and in this case:

$$N \to n\,N_o \equiv \;\; N_{HRR} \qquad (21)$$

since indeed also $\tau_3 \to 0$. Indeed:

$$\frac{1-e^{(n\tau_2/\tau)}}{1-e^{(\tau_2/\tau)}} \approx \frac{1-(1+n\tau_2/\tau)}{1-(1+\tau_2/\tau)} = \frac{-n\tau_2/\tau}{-\tau_2/\tau} = n \qquad (22)$$

We can therefore compare the actual number of measured radioisotopes N, to the number of radiosiotopes N_{HRR}, which would be obtained using a high-repetition laser in which $\tau_3 \approx 0$.

The ratio is given by:

$$\frac{N_{HRR}}{N} = \frac{nN_o}{N_o e^{-(\tau_3/\tau)}} \cdot \frac{1-e^{(\tau_2/\tau)}}{1-e^{(\tau_3/\tau)}} = ne^{+(\tau_3/\tau)} \cdot \frac{1-e^{(\tau_2/\tau)}}{1-e^{(\tau_3/\tau)}} \qquad (23)$$

https://doi.org/10.1017/hpl.2024.92 Published online by Cambridge University Press

Now taking into account the decay between the decay during the time τ_1 between the end of the irradiation and the beginning of the measurements, this number must also be increased by the factor $N_o e^{(\tau_1/\tau)}$. Finally, in the case of ^{44}Sc, we have:

$$n = 30, \qquad \tau_3 = 30\ min, \qquad \tau_2 = 1\ min, \qquad \tau = 343.7\ min$$

$$\frac{N_{HRR}}{N} = 30 \cdot e^{+(30/344)} \frac{1 - e^{(1/344)}}{1 - e^{(30/344)}} = 30 \cdot 1.09 \ \frac{-0{,}00291}{-0.091} = 1.05 \qquad (24)$$

which is a moderate increase.
Instead for the case of ^{11}C for which *$T_{1/2}$ = 20.4 min* (τ *=29,44 min*), we have:

$$n = 30, \qquad \tau_3 = 60\ min, \qquad \tau_2 = 2\ min, \qquad \tau = 29.44\ min$$

$$\frac{N_{HRR}}{N} = 30 \cdot e^{+(60/29.44)} \frac{1 - e^{(2/29.44)}}{1 - e^{(60/29.44)}} = 30 \cdot 7.676 \ \frac{-0{,}0703}{-6.676} = 2.42 \qquad (25)$$

This shows that delivering 30 shots in a short time instead of 1 hour would have more than doubled the number of ^{11}C radioisotopes. Indeed, this is technically feasible because PW lasers like Vega3 can in principle work at 1Hz repetition frequency (provided they are also coupled to a HRR target assembly) and delivering 30 shots would then require only half a minute.

Appendix B: Calculation of reaction products

A calculation of number of nuclear reactions taking place in the catcher can be performed using Monte Carlo simulations codes, like FLUKA or GEANT4. In order to allow for a faster and qualitatively correct estimation, we have developed a simpler software tool in python [49] which can be used to perform yield estimation for pitcher-catcher experiments, and which has been validated against the results of more complex (and time consuming) Monte Carlo Simulations.
This software, named FISP (for Fast Ion Spectrum Propagator), works in 1D using reaction cross-section and stopping power data, and assumes as input data the experimental spectrum of incident ions (in our case TNSA accelerated protons). This proton spectrum, divided in many quasi-monoenergetic contributions (bin) is propagated into the catcher target divided in infinitesimal slices.
In each slice, the energy deposited in the catcher from each bin in the spectrum is calculated according to the stopping power of the material at the corresponding bin energy. FISP uses Bethe's formula at high energies and a constant slowing down approximation at low energies. The limit is dynamically set by the code at the value of the peak of the stopping power curve calculated using Bethe's formula. The deposited energy is then removed from the initial energy to calculate the new bin energy. Any spectrum bin for which the energy falls to zero is removed from the spectrum, which is equivalent to particles stopping.
At the same time, for each energy bin and in each target slice, FISP calculates the number of reactions between the propagating protons and the different atoms in the catcher material. This is done using cross-section data.
FISP is not a Monte-Carlo code: it does not calculate the behavior of individual particles and repeat the calculations for many particles. Instead, for a population of particles it calculates the exact proportion of particles that will (or will not) react. Once the number of reactions is calculated, FISP removes one incident ion per reaction from the incident spectrum. The new population of ions

https://doi.org/10.1017/hpl.2024.92 Published online by Cambridge University Press

created by the reaction can eventually also be propagated into the target following a similar procedure. Since the code is 1D, the generated ions can only propagate back or forward. This process is repeated until the last slice of the target is allowing to calculate the spectrum of particles that exit the target on the front and on the back side. While clearly the 1D approximation does not allow to calculate angular distributions, we verified that it does not drastically affect the total number of generated particles nor the number of particles exiting the target.

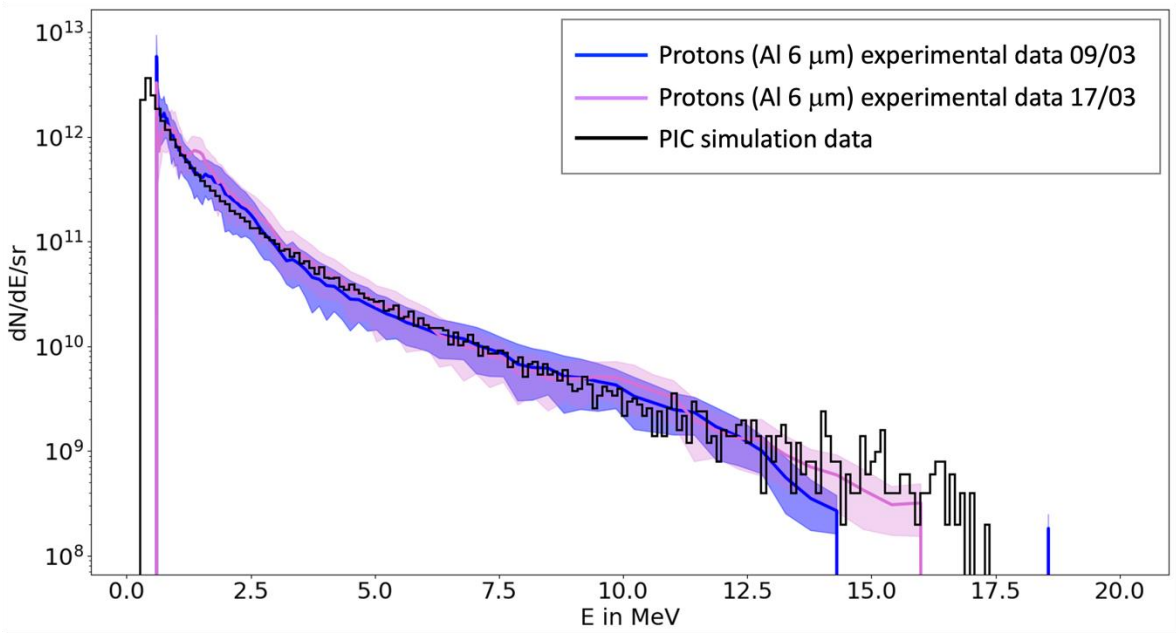

Fig. 11: Proton spectrum obtained with the Smilei PIC code and comparison with the experimental proton spectra measured with the TP.

Here we will detail the FISP calculations for the BNH_6 target with thickness 1.2 mm. The input proton spectrum used in the calculations is shown in Fig. 11. Two experimental spectra (to show shot-to-sot variations in the experiment) are shown and compared to a simulated spectrum.
The experimental spectra show a proton cut-off energy of the order of 15-17 MeV. The simulated spectra have been obtained by PIC simulations using the code SMILEI [50] assuming a pre-plasma density scale length of 0.1 μm as produced by the laser pedestal [51]. The spectra are shown per unit solid angle. The total numbers of protons have then been inferred by assuming a typical opening angle of the proton beam of ≈ 30° (half width).

The stopping power for BNH_6 has been calculated, as said, using Bethe's formula with the correct density of BNH_6 and an effective potential corresponding to the average chemical composition. The cross-section data for hydrogen boron fusion and for the generation of neutrons, and ^{11}C isotopes are taken from [52] and shown in Fig. 12.

https://doi.org/10.1017/hpl.2024.92 Published online by Cambridge University Press

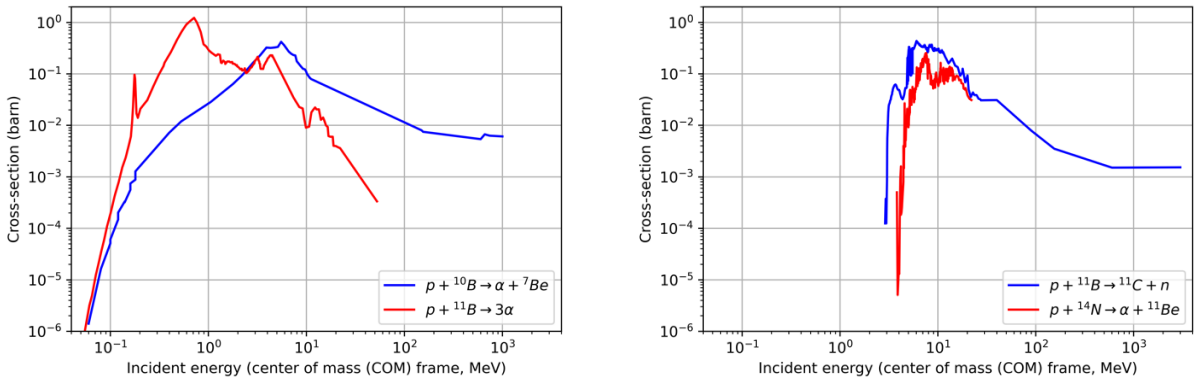

Fig. 12: The cross-section data for hydrogen boron fusion and for the generation of neutrons and ^{11}C isotopes.

Using such data, FISP calculates the total number of particles generated in the target, together with their spectra. ~~Fig. 13 shows the spectra of particles escaping the targets on front and rear side while~~ Table 4 shows the total number of particles generated, including those unable to exit the target. Fig. 13 shows the spectra of particles escaping the targets on front and rear side. In our case only about 1/10 of generated α-particles are able to escape the target (or $1.2 \cdot 10^6$), which is of course due to the very short penetration range of α-particles in solid density matter.

Created Ions	Number
α-particles	1.11e+07
^{7}Be	4.83e+05
neutrons	9.55e+05
^{11}C	9.55e+05

Tab. 4: Reaction products from ammonia borane.

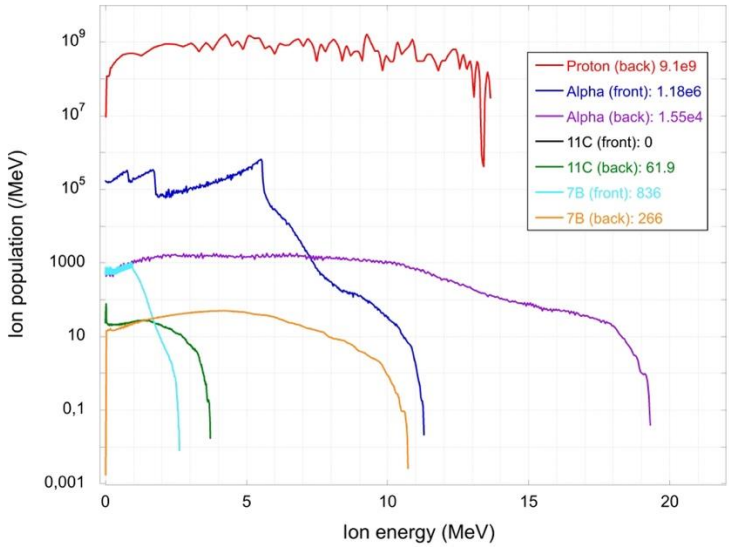

Fig. 13: The spectra of particles escaping the targets on front and rear side (results from FISP).

https://doi.org/10.1017/hpl.2024.92 Published online by Cambridge University Press

The number of ^{11}C and neutrons is the same since they are created by the same nuclear reaction. As for comparing the number of ^{11}C and α-particles, Fig. 12 shows that the maximum cross section for the two reactions is similar ($\approx$ 1 barn) but while the hydrogen-boron fusion cross section becomes already significant at energies as low as ≈ 100 keV (and reaches its maximum at ≈ 600 keV), the reaction generating ^{11}C requires proton energy to be > 2.765 MeV [52].
This means that low energy protons are effective in inducing a particle generation, but do not contribute to generating ^{11}C. Hence because of the low energy part of proton spectrum, we expect that the number of ^{11}C is much smaller than that of α–particles. Indeed, from the spectrum in Fig. 11 we can calculate a total number of protons (per unit solid angle) of $\approx 2.1 \cdot 10^{12}$, and a number of protons with E > 2.765 MeV which is $\approx 1.9 \cdot 10^{11}$. Hence there is a factor $\approx$ 10 between the two populations. Now the number of hydrogen boron fusion reaction from table 4 is $\approx 4 \cdot 10^{6}$ (1 reaction produces 3α) which is exceeding by a factor of $\approx$4 the production of ^{11}C. The remaining difference is due to the details of the cross sections.

Appendix C: CR39 measurements for ammonia borane

Solid state Nuclear Track detectors (CR39) have been used as detectors of α–particle generation. These plastic foils are exposed to the flux of particles generated from the interaction. The incoming radiation produces local damages by breaking of the long polymer chains. Along these damaged regions, the material is more susceptible to chemical attack, and, after a proper etching, holes become visible. These tracks can be properly characterized by microscope imaging providing information on particle energy and on type. For energies above ~ 1MeV, the hole size increases with the duration of the etching procedure and decreases when the α–particles energy increases [40]. In our experiment [37], after irradiation, the plastic polymer is etched in a caustic solution (6M NaOH at 70° for one or two hours).
In our experiment we used several CR39 foils placed in various position. However here we only describe the results obtained with the CR39 detector placed behind the TNSA shielding, as shown in Fig. 1. This shield prevented protons and other ions directly emitted from the pitcher to reach the CR39. However, in addition to α particles, other ions can be emitted from the catcher as a consequence of other nuclear reactions and, also, protons and ions from the pitcher can be scattered from the catcher and reach the CR39 detector. These can result in the production of holes in the etched CR39 which cannot easily be discriminated from those produced by α-particles. For this reason, half of CR39 was covered with a 5 µm Al foil. The goal of this Al foil was to stop ions which can arrive to the detector. However, it also filtered all α-particles with energies < 1.57 MeV.

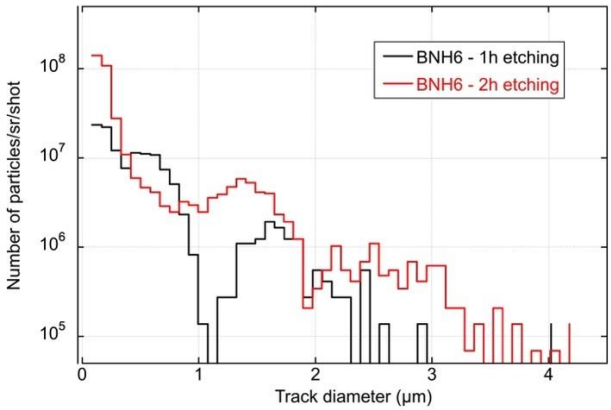

https://doi.org/10.1017/hpl.2024.92 Published online by Cambridge University Press

Fig. 14: Histogram obtained from CR39 in the case of irradiation of ammonia borane target. Here the CR39 was covered by a 5 μm Al filter.

Fig. 14 shows the histogram representing the number of holes (i.e. the number of particles) vs. hole diameter obtained from the analysis of CR39 foils corresponding to the irradiation of ammonia borane. Here, we identify the small holes as due to protons, while bigger holes correspond to α-particles and heavier ions. These bigger holes appear as a second peak in Fig.14, between 1.1 and 2.6 μm for 1 hour etching and between 2 and 3.6 μm for 2 hours etching. These correspond to α-particle energies from ∼0 up to ∼3.2 MeV. The correspondence between track diameter and α-particle energy follows an in-house calibration performed using the AIFIRA accelerator in Gradignan and a Plutonium source [53]. The limits of applicability of such identification methodology are described in detail in M. Scisciò et al. [36].

Finally, the summation of this α peak (for both 1 or 2 hours etching) provides a number of $\approx 5 \cdot 10^5$ α-particles per solid angle and per laser shot in the region covered by the 5 μm Al foil. By comparison in the region without filters we get $\approx 7 \cdot 10^6$ α-particles per solid angle and per laser shot, which, as explained, is over-estimated because without the Al filter, the CR39 is directly exposed to the particle flux and, in addition to α–particles, other ions can also reach the detector. The number of $5 \cdot 10^5$ α-particles of energy >1.57 MeV is instead more reliable, although some contamination from other laser accelerated ions cannot be completely excluded [36]. Assuming an isotropic generation over the 2π solid angle corresponding to the "front side", we can estimate $3 \cdot 10^6$ α-particles of energy >1.57 MeV.

References

1 A.Macchi, A.Antonicci, S.Atzeni, D.Batani, F.Califano, F.Cornolti, J.J.Honrubia, T.V.Lisseikina, F.Pegoraro and M. Temporal "Fundamental issues in fast ignition physics: from relativistic electron generation to proton driven ignition" Nuclear Fusion, 43 (May 2003) 362-368 (2003)

2 Hiroyuki Daido, Mamiko Nishiuchi, and Alexander, S. Pirozhkov "Review of laser-driven ion sources and their applications" Reports on Progress in Physics, Volume 75, Number 5 (2012) 056401DOI 10.1088/0034-4885/75/5/056401

3 V. S. Belyaev, A. P. Matafonov, V. I. Vinogradov et al. "Observation of neutronless fusion reactions in picosecond laser plasmas" Physical Review E - Statistical Physics, Plasmas, Fluids, and Related Interdisciplinary Topics, vol. 72, Article ID 026406, 2005

4 S. Kimura, A. Anzalone, and A. Bonasera "Comment on "Observation of neutronless fusion reactions in picosecond laser plasmas"", Physical Review E 79, 038401 (2009)

5 K. Batani, "Perspectives on research on laser driven proton-boron fusion and applications" JINST 18, C09012 (2023)

6 V. S. Belyaev, V. P. Krainov, A. P. Matafonov, and B. V. Zagreev, "The new possibility of the fusion p + ^{11} B chain reaction being induced by intense laser pulses" Laser Physics Letters, vol. 12, no. 9, Article ID 096001, 2015

7 M. Oliphant and E. Rutherford "Experiments on the transmutation of elements by protons" Proceedings of the Royal Society of London A, 141, 259 (1933)

8 Shizheng Zhang , Hao Xu, Xing Xu, Wenqing Wei, Jieru Ren, Benzheng Chen, Bubo Ma, Zhongmin Hu, Fangfang Li, Lirong Liu, Mingzhe Yang, Zeyu Lai, Hongwei Yue, Jie Xiong, Zhongfeng Xu, Yanhong Chen, Zhao Wang, Zexian Zhou, Lulin Shi, Rui Cheng, Zhigang Deng, Wei Qi, Weimin Zhou, Guanchao Zhao, Bing Liu, Di Luo, Dieter H. H. Hofmann, and Yongtao Zhao "Cross-Section Measurements of the ^{11}B$(p,\alpha)2\alpha$ Reaction near the First Resonant Energy" Laser Part. Beams 2023 (2023) 9697329

9 A. Picciotto, D. Margarone, A. Velyhan, P. Bellutti, J. Krasa, A. Szydlowsky, G. Bertuccio, Y. Shi, A. Mangione, J. Prokupek, A. Malinowska, E. Krousky, J. Ullschmied, L. Laska, M. Kucharik, and G. Korn "Boron-Proton Nuclear-Fusion Enhancement Induced in Boron-Doped Silicon Targets by Low-Contrast Pulsed Laser" Physical Review X 4, 031030 (2014)

https://doi.org/10.1017/hpl.2024.92 Published online by Cambridge University Press

[10] D Margarone, A Picciotto, A Velyhan, J Krasa, M Kucharik, A Mangione, A Szydlowsky, A Malinowska, G Bertuccio, Y Shi, M Crivellari, J Ullschmied, P Bellutti and G Korn "Advanced scheme for high-yield laser driven nuclear reactions" Plasma Phys. Control. Fusion 57 014030 (2015)

[11] L. Giuffrida, F. Belloni, D. Margarone, G. Petringa, G. Milluzzo, V. Scuderi, A. Velyhan, M. Rosinski, A. Picciotto, M. Kucharik, J. Dostal, R. Dudzak, J. Krasa, V. Istokskaia, R. Catalano, S. Tudisco, C. Verona, K. Jungwirth, P. Bellutti, G. Korn, and G. A. P. Cirrone, "High-current stream of energetic a particles Phys. Rev. E 101, 013204 (2020)

[12] D. Margarone, J. Bonvalet, L. Giuffrida, A. Morace, V. Kantarelou, M. Tosca, D. Raffestin, P. Nicolaï, A. Picciotto, Y. Abe, Y. Arikawa, S. Fujioka, Y. Fukuda, Y. Kuramitsu, H. Habara, and D. Batani, In-target proton-boron nuclear fusion using a PW-class laser, Applied Sciences, 12, 1444 (2022)

[13] C. Labaune, C. Baccou, S. Depierreux, C. Goyon, G. Loisel, V. Yahia, and J. Rafelski, "Fusion reactions initiated by laser-accelerated particle beams in a laser-produced plasma", Nat. Commun. 4, 2506 (2013).

[14] C. Baccou, V. Yahia, S. Depierreux, C. Neuville, C. Goyon, F. Consoli, R. De Angelis, J. E. Ducret, G. Boutoux, J. Rafelski, and C. Labaune "CR-39 track detector calibration for H, He, and C ions from 0.1-0.5 MeV up to 5 MeV for laser-induced nuclear fusion product identification", Review of Scientific Instruments, 86, 083307 (2015)

[15] D. Margarone, A. Morace, J. Bonvalet, Y. Abe, V. Kantarelou, D. Raffestin, L. Giuffrida, P. Nicolai, M. Tosca, A. Picciotto, G. Petringa, G. A. P. Cirrone, Y. Fukuda, Y. Kuramitsu, H. Habara, Y. Arikawa, S. Fujioka, E. D'Humieres, G. Korn, and D. Batani, "Generation of a-particle beams with a multi-kJ, Peta-Watt class laser system" Frontiers in Physics, 8, 343 (2020)

[16] J. Bonvalet, P. Nicolaï, D. Raffestin, E. D'humieres, D. Batani, V. Tikhonchuk, V. Kantarelou, L. Giuffrida, M. Tosca, G. Korn, A. Picciotto, A. Morace, Y. Abe, Y. Arikawa, S. Fujioka, Y. Fukuda, Y. Kuramitsu, H. Habara, and D. Margarone, "Energetic a-particle sources produced through proton-boron reactions by high-energy high-intensity laser beams", Phys. Rev. E 103, 053202 (2021)

[17] F. Lindau, O. Lundh, A. Persson, P. McKenna, K. Osvay, D. Batani, and C.-G. Wahlström "Laser-Accelerated Protons with Energy-Dependent Beam Direction" Physical Review Letters, 95, 175002 (2005)

[18] V. Malka, J. Faure, S. Fritzler, M. Manclossi, A. Guemnie-Tafo, E. d'Humières, E. Lefebvre, D. Batani; Production of energetic proton beams with lasers. Rev. Sci. Instrum., 77, 03B302 (2006)

[19] D. Batani, G. Boutoux, F. Burgy, K. Jakubowska, and J. E. Ducret "Proton acceleration measurements using fs laser irradiation of foils in the target normal sheath acceleration regime" Phys. Plasmas, Physics of Plasmas 25, 054506 (2018)

[20] A. Macchi, M. Borghesi, and M. Passoni, "Ion acceleration by superintense laser-plasma interaction" Rev. Mod. Phys. 85, 751 (2013)

[21] M. Passoni, C. Perego, A. Sgattoni, D. Batani "Advances in target normal sheath acceleration theory" Phys. Plasmas 20(6), 060701 (2013)

[22] Francesco Ingenito, Pierluigi Andreoli, Dimitri Batani, Aldo Bonasera, Guillaume Boutoux, Frederic Burgy, Mattia Cipriani, Fabrizio Consoli, Giuseppe Cristofari, Riccardo De Angelis, Giorgio Di Giorgio, Jean Eric Ducret, Danilo Giulietti, and Katarzyna Jakubowska "Directional Track Selection Technique in CR39 SSNTD for low- yield reaction experiments" EPJ Web of Conferences 167, 05006 (2018)

[23] Fabrizio Consoli, Riccardo De Angelis, Pierluigi Andreoli, Aldo Bonasera, Mattia Cipriani, Giuseppe Cristofari, Giorgio Di Giorgio, Danilo Giulietti and Martina Salvadori "Diagnostic Methodologies of Laser-Initiated ^{11}B(p,α)2α Fusion Reactions" REVIEW article, Front. Phys., November, Volume 8, 561492 (2020) https://doi.org/10.3389/fphy.2020.561492

[24] Martina Salvadori, Massimiliano Scisciò, Giorgio Di Giorgio, Mattia Cipriani, Pier Luigi Andreoli, Giuseppe Cristofari, Riccardo De Angelis, Danilo Giulietti, and Fabrizio Consoli "Univocal Discrimination of α Particles Produced by ^{11}B(p, α)2α Fusions in Laser-Matter Experiments by Advanced Thomson Spectrometry" Laser Part. Beams 2023 7831712 (2023)

[25] M. Scisciò, G. Di Giorgio, P. L. Andreoli, M. Cipriani, G. Cristofari, R. De Angelis, M. Salvadori, G. A. P. Cirrone, L. Giufrida, D. Margarone, G. Milluzzo, G. Petringa, and F. Consoli "High-Sensitivity Thomson Spectrometry in Experiments of Laser-Driven Low-Rate NeutronLess Fusion Reactions", Laser Part. Beams 2023 (2023) 3531875

[26] Marius S. Schollmeier , Vahe Shirvanyan, Christie Capper, Sven Steinke, Adam Higginson, Reed Hollinger, John T. Morrison, Ryan Nedbailo, Huanyu Song, Shoujun Wang, Jorge J. Rocca, and Georg Korn "Investigation of Proton Beam-Driven Fusion Reactions Generated by an Ultra-Short Petawatt-Scale Laser Pulse" Laser Part. Beams Volume 2022, Article ID 2404263, (2022)

[27] M. R. D. Rodrigues, A. Bonasera, M. Scisciò, J. A. Pérez-Hernández, M. Ehret, F. Filippi, P. L. Andreoli, M. Huault, H. Larreur, D. Singappuli, D. Molloy, D. Raffestin, M.Alonzo, G. G. Rapisarda, D. Lattuada, G. L. Guardo, C. Verona, Fe. Consoli, G. Petringa, A. McNamee, M. La Cognata, S. Palmerini, T. Carriere, M. Cipriani, G. Di Giorgio, G.Cristofari, R. De Angelis, G. A. P. Cirrone, D. Margarone, L. Giuffrida, D. Batani, P.Nicolai, K. Batani, R. Lera, L. Volpe, D. Giulietti, S. Agarwal, M. Krupka, S. Singh, Fa.Consoli "Radioisotopes production using lasers: from basic science to applications" Matter and Radiation at Extremes Matter Radiat. Extremes 9, 037203 (2024) https://doi.org/10.1063/5.0196909

https://doi.org/10.1017/hpl.2024.92 Published online by Cambridge University Press

[28] A. Maffini, F. Mirani, A. C. Giovannelli, A. Formenti, M. Passoni "Laser-driven production with advanced targets of Copper-64 for medical applications", Frontiers in Physics 11 (2023) https://doi.org/10.3389/fphy.2023.1223023

[29] Katarzyna Szkliniarz, Mateusz Sitarz, Rafał Walczak, Jerzy Jastrzębski, Aleksander Bilewicz, Jarosław Choiński, Andrzej Jakubowski, Agnieszka Majkowska, Anna Stolarz, Agnieszka Trzcińska, Wiktor Zipper "Production of medical Sc radioisotopes with an alpha particle beam" Applied Radiation and Isotopes 118, 182 (2016)

[30] F. Haddad, L. Ferrer, G. Arnaud, T. Carlier, N. Michel, J. Barbet, and J.-F. Chatal, "ARRONAX, a high-energy and high-intensity cyclotron for nuclear medicine", Eur. J. Nucl. Med. Mol. Imaging 35, 1377 (2008)

[31] Institute of Nuclear Physics (Czech Academy of Sciences) in Řež near Prague: https://www.ujf.cas.cz/en/

[32] François Guérard, Jean-François Gestin, and Martin W. Brechbiel, « Production of [^{211}At] Astatinated Radiopharmaceuticals and Applications in Targeted α-Particle Therapy" Cancer Biother Radiopharm. Feb; 28(1): 1–20 (2013)

[33] R. Walczak, S. Krajewski, K. Szkliniarz, M. Sitarz, K. Abbas, J. Choiński, A. Jakubowski, J. Jastrzębski, A. Majkowska, F. Simonelli, A. Stolarz, A. Trzcińska, W. Zipper and A. Bilewicz "Cyclotron production of ^{43}Sc for PET imaging" EJNMMI Physics 2 (2015) 33.

[34] Seweryn Krajewski, Izabela Cydzik, Kamel Abbas, Antonio Bulgheroni, Federica Simonelli, Uwe Holzwarth and Aleksander Bilewicz "Cyclotron production of ^{44}Sc for clinical application" Radiochimica Acta https://doi.org/10.1524/ract.2013.2032

[35] https://www.euronuclear.org/news/radioisotopes-for-life-ensuring-european-supply-stakeholders-opportunities/ https://www.medraysintell.com/

[36] M. Scisciò, G. Petringa, Z. Zhe, M. R. D. Rodrigues, M. Alonzo, P. L. Andreoli, F. Filippi, Fe. Consoli, M. Huault, D. Raffestin, D. Molloy, H. Larreur, D. Singappuli, T. Carriere,C. Verona, P. Nicolai, A. McNamee, M. Ehret, E. Filippov, R. Lera, J. A. Pérez-Hernández, S. Agarwal, M. Krupka, S. Singh, D. Lattuada, M. La Cognata, G. L. Guardo, S. Palmerini, G. Rapisarda[2] K. Batani, M. Cipriani, G. Cristofari, E. Di Ferdinando, G. Di Giorgio, R. De Angelis, D. Giulietti, X. Jun, L. Volpe, L. Giuffrida, D. Margarone, D. Batani, G. A. P. Cirrone, A. Bonasera and Fa. Consoli, Laser-Initiated p-^{11}B fusion reactions in petawatt high-repetition-rates laser facilities, https://doi.org/10.48550/arXiv.2411.04577

[37] M. Huault, T. Carrière, H. Larreur, Ph. Nicolaï, D. Raffestin, D. Singappuli, E. D'Humieres, D. Dubresson, K. Batani, M. Cipriani, F. Filippi, M. Scisciò, C. Verona, L. Giuffrida, V. Kantarelou, S. Stancek, N. Boudjema, R. Lera, J.A. Pérez-Hernández, L. Volpe, M. D. Rodríguez Frías, A. Bonasera, M.R.D. Rodrigues, D. Ramirez Chavez, F. Consoli, and D. Batani, "Experimental and computational evaluation of Alpha particle production from Laser-driven proton-boron nuclear reaction in hole-boring scheme." Physics of Plasmas, accepted for publication (2024)

[38] Chris Spindloe and coworkers at SciTech Precision in UK.

[39] I.C.E. Turcu, D. Margarone, L. Giuffrida, A. Picciotto, C. Spindloe, A.P.L. Robinson and D. Batani, Borane (B_mH_n), Hydrogen rich, Proton Boron fusion fuel materials for high yield laser-driven Alpha sources, JINST 19 C03065 (2024)

[40] Vasiliki Kantarelou, Andriy Velyhan, Przemysław Tchórz, Marcin Rosiński, Giada Petringa , Giuseppe Antonio Pablo Cirrone, Valeriia Istokskaia, Josef Krása , Miroslav Krus , Antonino Picciotto , Daniele Margarone and Lorenzo Giuffrida, A Methodology for the Discrimination of Alpha Particles from other Ions in Laser-Driven Proton-Boron Reactions Using CR-39 Detectors Coupled in a Thomson Parabola Spectrometer, Laser and Particle Beams, Volume 2023, Article ID 3125787, 12 pages https://doi.org/10.1155/2023/3125787

[41] D. Dellasega, V. Russo, A. Pezzoli, C. Conti, N. Lecis, E. Besozzi, M. Beghi, C.E. Bottani, M. Passoni, "Boron films produced by high energy Pulsed Laser Deposition", Materials & Design 134 (2017). https://doi.org/10.1016/j.matdes.2017.08.025

[42] D. Mazzucconi, D. Vavassori, D. Dellasega, F.M. Airaghi, S. Agosteo, M. Passoni, A. Pola, D. Bortot, "Proton boron fusion reaction: A novel experimental strategy for cross section investigation", Radiat. Phys. Chem. 204 (2023). https://doi.org/10.1016/j.radphyschem.2022.110727

[43] David A. Rotsch, M. Alex Brown, Jerry A. Nolen, Thomas Brossard, Walter F. Henning, Sergey D. Chemerisov, Roman G. Gromov, John Greene "Electron linear accelerator production and purification of scandium-47 from titanium dioxide targets", Applied Radiation and Isotopes 131 (2018) 77–82

[44] Jacco Vink "Gamma-ray observations of explosive nucleaosynthesis products" Advances in Space reserarch, 35 (6) 976-986 (2005)

[45] DK Kaipov, YG Kosyak, YA Lysikov "Lifetimes of sup (40, 44) Ca excited levels" inis.iaea.org [from Russian: "ВРЕМЕНА ЖИЗНИ ВОЗБУЖДЕННЫХ УРОВНЕЙ (40, 44)" Д.К.Каипов,Ю.Г.Косяк,Ю.А.Лнсиков]

[46] https://en.wikipedia.org/wiki/Isotopes_of_scandium#:~:text=Naturally%20occurring%20scandium%20(21Sc,half%2Dlife%20of%203.97%20hours.

[47] https://www.clf.stfc.ac.uk/Pages/CALTA.aspx

[48] https://en.wikipedia.org/wiki/Calcium

https://doi.org/10.1017/hpl.2024.92 Published online by Cambridge University Press

[49] Howel Larreur, Thomas Carrière, Luca Volpe, Dimitri Batani "Optimisation of catcher target thickness in laser-driven proton-boron fusion experiments" 3rd International Workshop on Proton-Boron Fusion, Prague, October 2023

[50] J. Derouillat, A. Beck, F. P.rez, T. Vinci, M. Chiaramello, A. Grassi, M. Fl., G. Bouchard, I. Plotnikov, N. Aunai, J. Dargent, C. Riconda, and M. Grech, "Smilei : A collaborative, open-source, multi-purpose particlein-cell code for plasma simulation," Computer Physics Communications, vol. 222, pp. 351–373 (2018)

[51] Pierre-Henri Maire, Rémi Abgrall, Jérôme Breil, and Jean Ovadia "A Cell-Centered Lagrangian Scheme for Two-Dimensional Compressible Flow Problems" SIAM J. Sci. Comput., 29, 1781 (2007)

[52] https://www-nds.iaea.org/exfor/

[53] https://www.lp2ib.in2p3.fr/aifira/

[new_reference] Antonino Picciotto, Matteo Valt, Daniel P. Molloy, Andrea Gaiardo, Alessandro Milani, Vasiliki Kantarelou, Lorenzo Giuffrida, Gagik Nersisyan, Aaron McNamee, Jonathan P. Kennedy, Colm R.J. Fitzpatrick, Philip Martin, Davide Orecchia, Alessandro Maffini, Pietro Scauso, Lia Vanzetti, Ion Cristian Edmond Turcu, Lorenza Ferrario, Richard Hall-Wilton, Daniele Margarone "Ammonia borane-based targets for new developments in laser-driven proton boron fusion" Applied Surface Science Journal (2024) 672, 160797

https://doi.org/10.1017/hpl.2024.92 Published online by Cambridge University Press